ANNALI DI GEOFISICA, VOL. 42, N. 4, August 1999

Stress tensor inversion in Western Greece using earthquake focal mechanisms from the Kozani-Grevena 1995 seismic sequence

Anastasia A. Kiratzi
Department of Geophysics, Aristotle University of Thessaloniki, Greece

Abstract
Stress tensor inversion has been applied to estimate principal stress axes orientations in Western Greece, from 178 earthquake fault plane solutions from the Kozani-Grevena May 13, 1995 sequence. All focal mechanisms were previously determined through the deployment of a dense portable array. The magnitude range is 2.7-6.5 and the depth range is 4.0-15 km. A single stress tensor with an average misfit of 6.5°, small enough to support the assumption of stress homogeneity, can describe the stress field. The maximum compressive stress, σ_1, has a NNE-SSW trend (N26°E) and a nearly vertical plunge (80°) while the minimum compressive stress, σ_3, has a NNW-SSE orientation (N159°E) and a shallow plunge (7°) southwards. The scalar quantity, R (stress ratio) was found equal to 0.4 suggesting a transtensional regime (normal faulting with strike-slip motions) in which σ_2 is compressional. The identification of the fault plane from the auxiliary plane was achieved for 99 fault plane solutions out of 178 in total (56%). Vertical cross sections support previous results concerning the north dipping main fault segments and the south dipping antithetic faulting. The strike-slip motion is mainly dextral, along NNE-SSW structures, which follow the direction of the main neotectonic faults while the scarce sinistral strike-slip motion is connected to NW-SE trending zones of weakness pre-existing the old phase of compression in the Aegean. The strong strike slip motion that supports the transtensional regime probably reflects the effect of the motions of the North Anatolian Fault, taken up by normal faulting in the area of Western Greece.

Key words *stress distribution – inversion – fault plane solutions – Greece*

1. Introduction

On 13 May 1995 an earthquake of magnitude $M_w = 6.5$ occurred in Northwestern Greece (40.183°N - 21.660°E) in an epicentral area that was considered to be of low seismicity (Papazachos and Papazachou, 1997; B. Papazachos *et al.*, 1995, 1998; Stiros, 1998). The earthquake caused extensive damage in many villages located within the epicentral area and considerably affected the two largest cities, Kozani and Grevena. The earthquake sequence has been extensively studied and a series of publications are available to the reader (Pavlides *et al.*, 1995; Mountrakis *et al.*, 1995, 1998; B. Papazachos *et al.* 1995, 1998; Clarke *et al.* 1996; Chiarabba and Selvaggi, 1997; C. Papazachos *et al.* 1998; Hatzfeld *et al.* 1997, 1998; Papanastassiou *et al.*, 1998; Pavlides and King, 1998).

All the studies conclude that the sequence was due to a normal fault striking ENE-WSW and dipping to NNW with an angle of 35°-45° with the mainshock generated in the central, deepest part of the fault under the ophiolites of Mount Vourinos. The epicentral area (fig. 1) lies in the western margin of the Pelagonian zone

Mailing address: Prof. Anastasia A. Kiratzi, Department of Geophysics, Aristotle University of Thessaloniki, 540 06 Thessaloniki, Greece; e-mail: Kiratzi@geo.auth.gr

(Mountrakis, 1986). Neotectonic studies have shown that the area is dominated by NE-SW trending neotectonic active faults, one of these being the Aliakmon River Fault that forms the exit of the river to the Aegean Sea (Pavlides and Mountrakis, 1987; Pavlides and Simeakis, 1988). At the area of Lake Polifitos two fault segments are identified, the Servia Fault that remained inactive during the sequence and the segment of Rimnio-Paleohori-Sarakina-Nisi which is the main seismogenic fault of the 1995 event. This fault was identified by field studies conducted after the occurrence of the mainshock (Mountrakis *et al.*, 1995). It has a length of about 30 km, a NE-SW strike and a NW dip. The clearest evidence of the fault was the surface traces at the area of Paleohori-Sarakina-Nisi covering a distance of ~ 15 km. Antithetic faulting having the same strike but dipping to SE was observed at the same area (Mountrakis *et al.*, 1998), mainly along the traces of Chromio-Myrsina (fig. 1). This antithetic faulting is probably connected to the Aliakmon River Fault at the site of Rimnio (Pavlides, 1998). Both the Servia Fault and the Paleohori Fault segments are characterized by a very large return period of ~2000-4000 years for earthquakes of M 6 up to 6.8.

In the present study we use a data set of 177 fault plane solutions of aftershocks (all determined by Hatzfeld *et al.*, 1997) as well as the focal mechanism of the 1995 mainshock, determined by inversion by the Geological Survey of Japan (GSJ), to invert for the present stress regime acting in Western Greece.

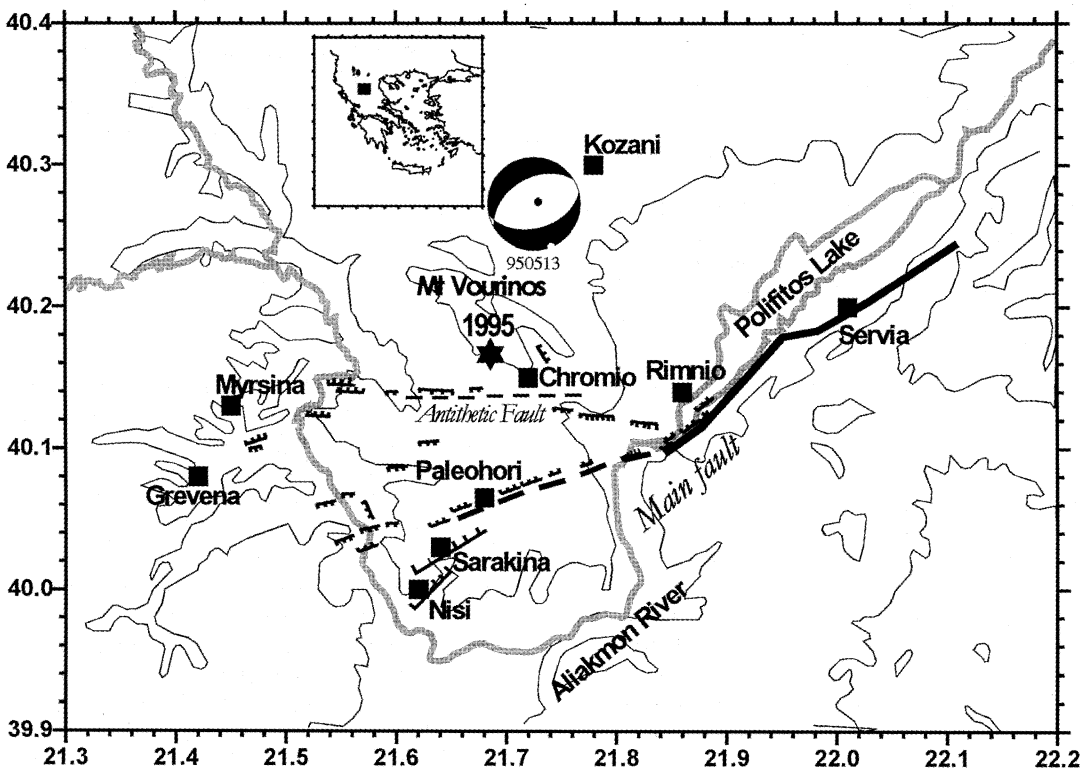

Fig. 1. The Kozani-Grevena area with the main geological faults. The surface ground ruptures of the main fault (Paleohori-Sarakina-Nisi), the antithetic fault (Chromio-Myrsina) as well as the focal mechanism of the mainshock are also shown.

2. Stress tensor inversion

2.1. *Method*

The directions of the stress tensor were calculated following the Gephart and Forsyth (1984) and Gephart (1990) method. The basic assumptions of this method are: a) the deviatoric stress is uniform over a given rock volume and time interval; b) earthquakes are shear dislocations on pre-existing faults and c) slip occurs in the direction of the resolved shear stress on the fault plane. The last condition is fully satisfied if the slip direction on a plane of any focal mechanism is aligned with the direction of the resolved shear stress.

The algorithm inverts for the orientation of the stress principal axes σ_1, σ_2, and σ_3 (maximum, intermediate and minimum stress respectively) and the parameter R $\{= (\sigma_2 - \sigma_1)/(\sigma_3 - \sigma_1)\}$ which gives a relative measure of stress magnitudes and constrains the shape of the stress ellipsoid. The inversion scheme tries to minimize the differences between the slip direction, computed from the stress tensor and the observed slip on each plane of the focal mechanisms. The difference between the computed slip and the observed slip is evaluated through an angular rotation (misfit), F, about an arbitrary axis. Thus, the misfit is the minimum rotation that brings the slip of one of the two nodal planes to match the resolved shear stress tensor. It is calculated through a grid search, systematically varying the orientation of the principal stresses and the parameter R. The stress tensor that corresponds to the minimum average rotation angle is assumed to be the best stress tensor for the specific population of focal mechanisms.

Gephart and Forsyth (1984), assuming that all the misfits follow a Gaussian distribution around the minimum misfit, found that the $L1$ norm is an appropriate measure of the misfit on the grounds that it limits the effects of any poorly fitting data. The quality of the inversion is evaluated through the calculation of the 95% confidence limits of the best fitting model as described in Parker and McNutt (1980) and Gephart and Forsyth (1984), according to the expression

$$\sum_{95} = \left(\frac{1.96(\pi/2-1)^{1/2} n^{1/2} + n}{n-k} \right) \sum_{\min} \quad (2.1)$$

where $\sum_{min} = F$, *i.e.* the minimum average rotation angle, n is the number of the focal mechanisms used and k is the number of the variables of the model. The number of variables is 4 in this case, that is 3 principal stress directions (Euler angles) and the stress ratio, R. This test gives us an expression of the confidence limit once we have found the best-fitting model.

The value of the average misfit corresponding to the best stress model provides a guide as to how well the assumption of stress homogeneity is fulfilled, in relation to the seismic sample submitted to inversion (Michael, 1987). In a series of tests carried out by Wyss *et al.* (1992) it was found in the case of homogeneous stress, errors in the data (focal mechanisms) of the order of 5°, 10°, and 15° were associated with misfit values not larger than 3°, 6°, and 8°, respectively.

2.2. *Results*

From the 178 focal mechanisms submitted in the inversion only the fault plane of the mainshock was assumed known *a priori*, on the basis of previous studies (Pavlides *et al.*, 1995; Hatzfeld *et al.*, 1997, 1998; B. Papazachos *et al.*, 1995, 1998). Aftershock magnitudes ranged from 2.7-4.4. All data were equally weighted, w = 1, except the mainshock which was assigned a w = 2. The aftershock focal mechanisms were all determined by more than 20 polarity readings (Hatzfeld *et al.*, 1997) so we assumed that they were all determined with errors in the strike, dip and rake no more than 10°.

The resulting stress tensor, as listed in table I, shows an extensional regime, with a nearly vertical σ_1, with σ_2 trending SW-NE and 7° plunging to the SW, and σ_3 trending NW-SE and 7° plunging to the SE. The minimum average misfit, F is 6.5° and the value of R is 0.4. Following our previous discussion, given the F value obtained, and the assumed error in the fault plane solutions (~ 10°), we conclude that the stress

homogeneity criterion is fulfilled and no further attempt was made to invert for smaller subsets. The value of the stress ratio (R = 0.4) corresponds to a normal faulting regime, combined with strong strike-slip motion, in which σ_2 is compressional (Bellier *et al.*, 1997).

Figure 2 shows the distribution of misfit rotation angles for every individual earthquake. Any individual misfits greater than 20° (only six) may be assumed to prove inconsistency between the focal mechanism and the resolved stress tensor. The mainshock (No. 1 in fig. 2) has a very small

Table I. Stress tensor inversion results for the earthquakes of Western Greece.

Average misfit, F	σ_1		σ_2		σ_3		R	N
	Dip	Strike	Dip	Strike	Dip	Strike		
6.5°	80°	26°	7°	250°	7°	159°	0.4	178

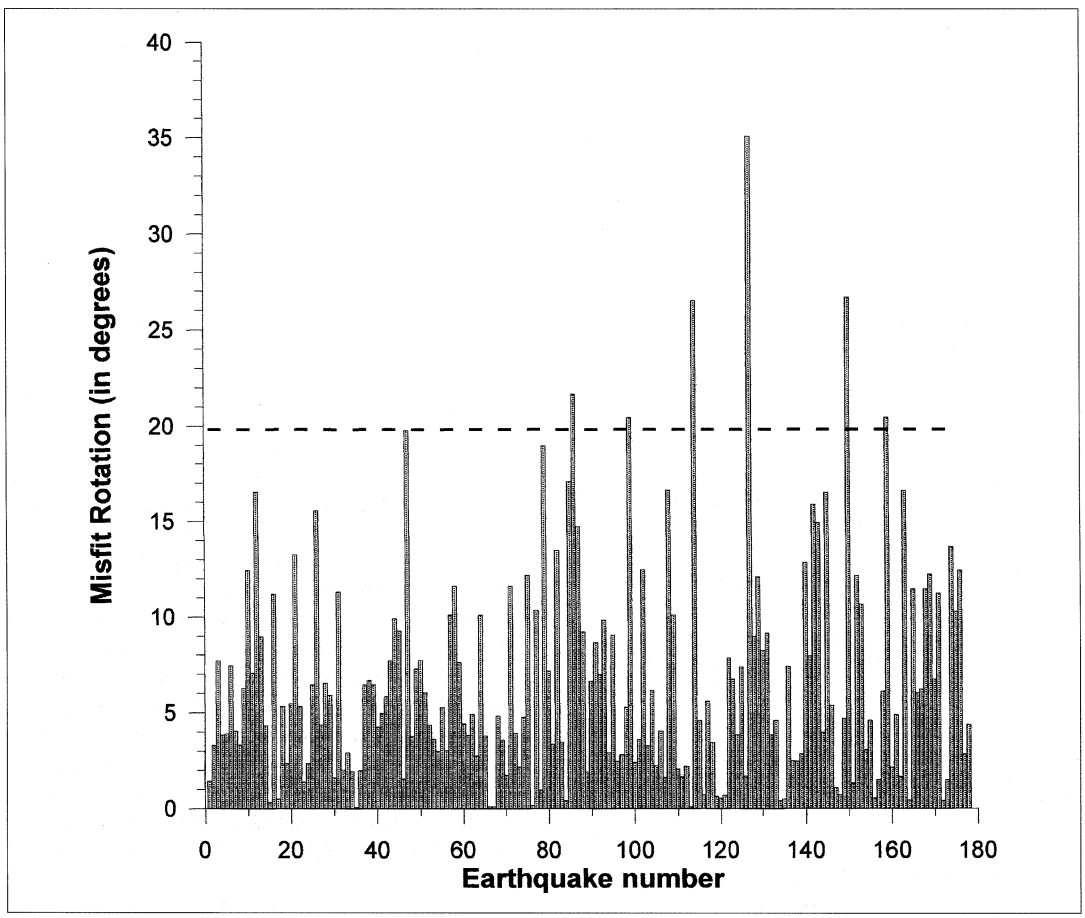

Fig. 2. Distribution of earthquake individual misfits (in degrees) computed with respect to the best stress model (misfit rotation angle *versus* number of earthquake, No. 1 is the mainshock).

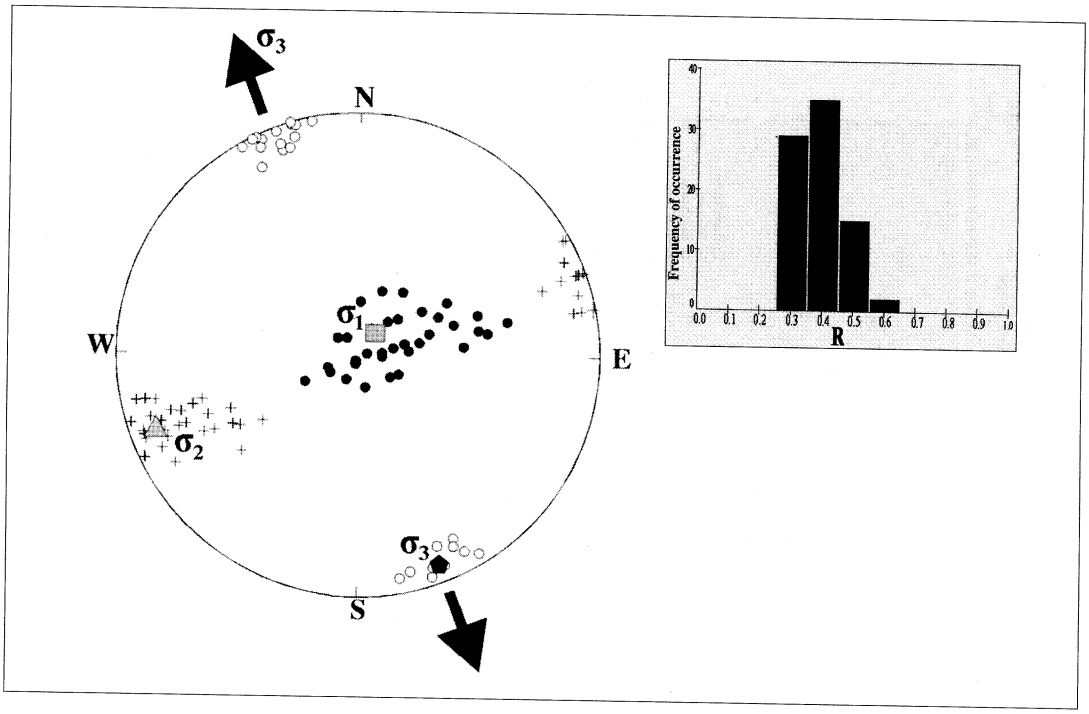

Fig. 3. Orientation of principal stresses in Western Greece, together with the 95% confidence limits for σ_1, σ_2 and σ_3. The inset shows the distribution of R within the 95% confidence models.

misfit (1.45°) relative to the best stress model suggesting that this event did not perturb the stresses in the region, that is, the stresses affecting the mainshock were the same as those felt by the aftershocks. Plots of the variation of the earthquake individual misfit *versus* depth and longitude revealed no systematic trend.

Figure 3 shows the 95% confidence limits evaluated for the best-fitting model, (from eq. (2.1) with $n = 178$, $k = 4$ and $\Sigma_{min} = 6.5°$), and it is seen that the stress tensor is well resolved as the areas defined on the stereonet by the limits of the orientations of σ_1 and σ_3 do not overlap.

3. Identification of the fault plane from the two nodal planes

According to Gephart and Forsyth (1984) the actual failure plane of each focal mechanism has a smaller misfit than the auxiliary plane. They consider a good fitting to the data when the actual fault plane has an angular rotation of less than 20° and the differences in angular rotation between the two nodal planes is greater than 10°. With these conditions, from the 177 focal mechanisms of the aftershocks we were able to identify a preferred fault plane from the auxiliary plane in 98 cases. For 79 solutions this was not possible because the difference in angular rotations between the two planes was less than 10°. Thus, only these focal mechanism solutions for which the fault plane could be unambiguously determined were further used to investigate the information they give in comparison to the previous knowledge about the fault that caused the Kozani-Grevena earthquake.

Figure 4a-d shows the focal mechanisms of those earthquakes for which the fault plane could be unambiguously identified. They were

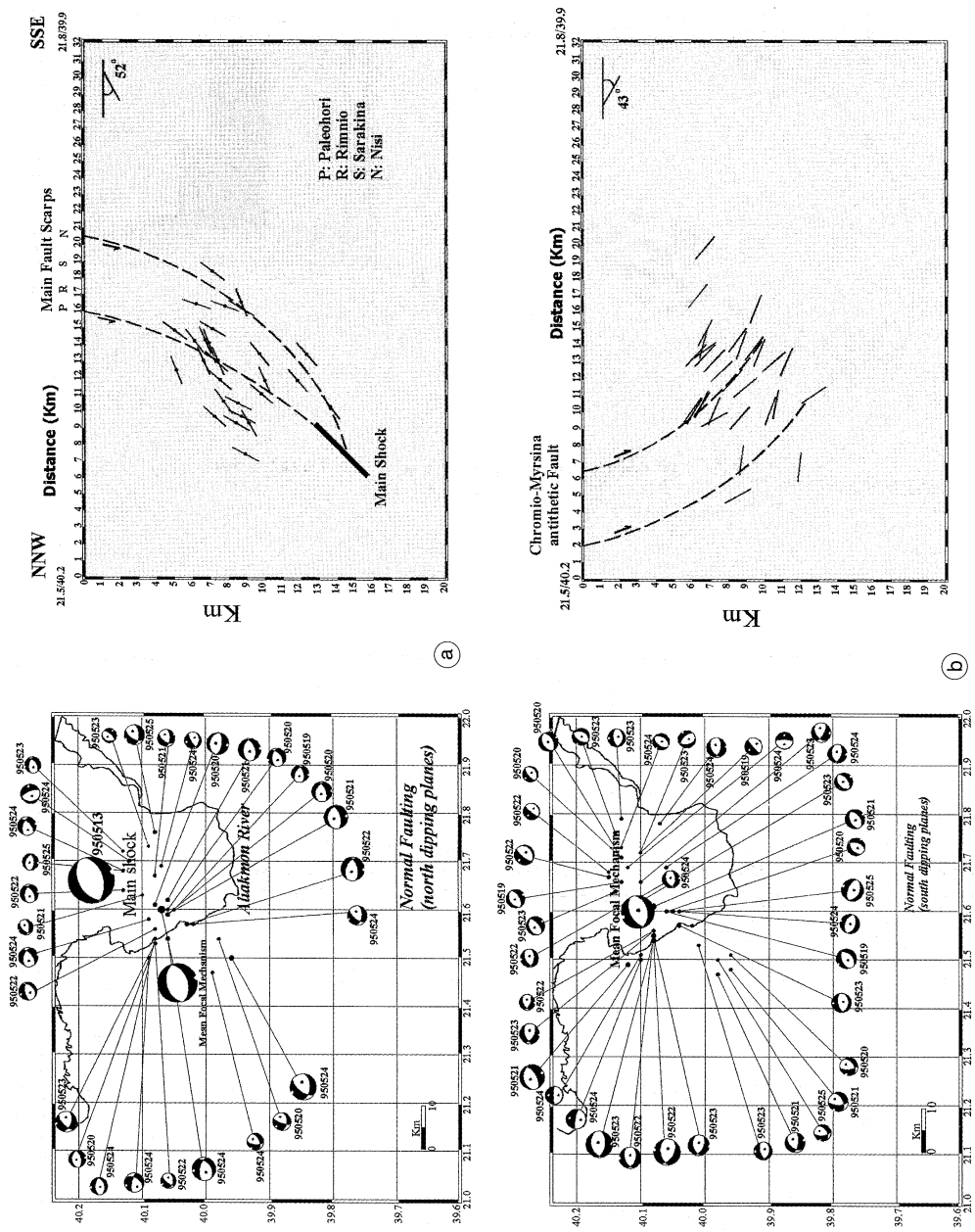
NNW
Distance (Km)
SSE
Main Fault Scarps
P R S N
52°
P: Paleohori
R: Rimnio
S: Sarakina
N: Nisi
Main Shock
Km
21.5/40.2
21.8/39.9
a
Chromio-Myrsina
antithetic Fault
43°
b
950513
Main Shock
Aiakhrom River
Mean Focal Mechanism
Normal Faulting
(north dipping planes)
Normal Faulting
(south dipping planes)

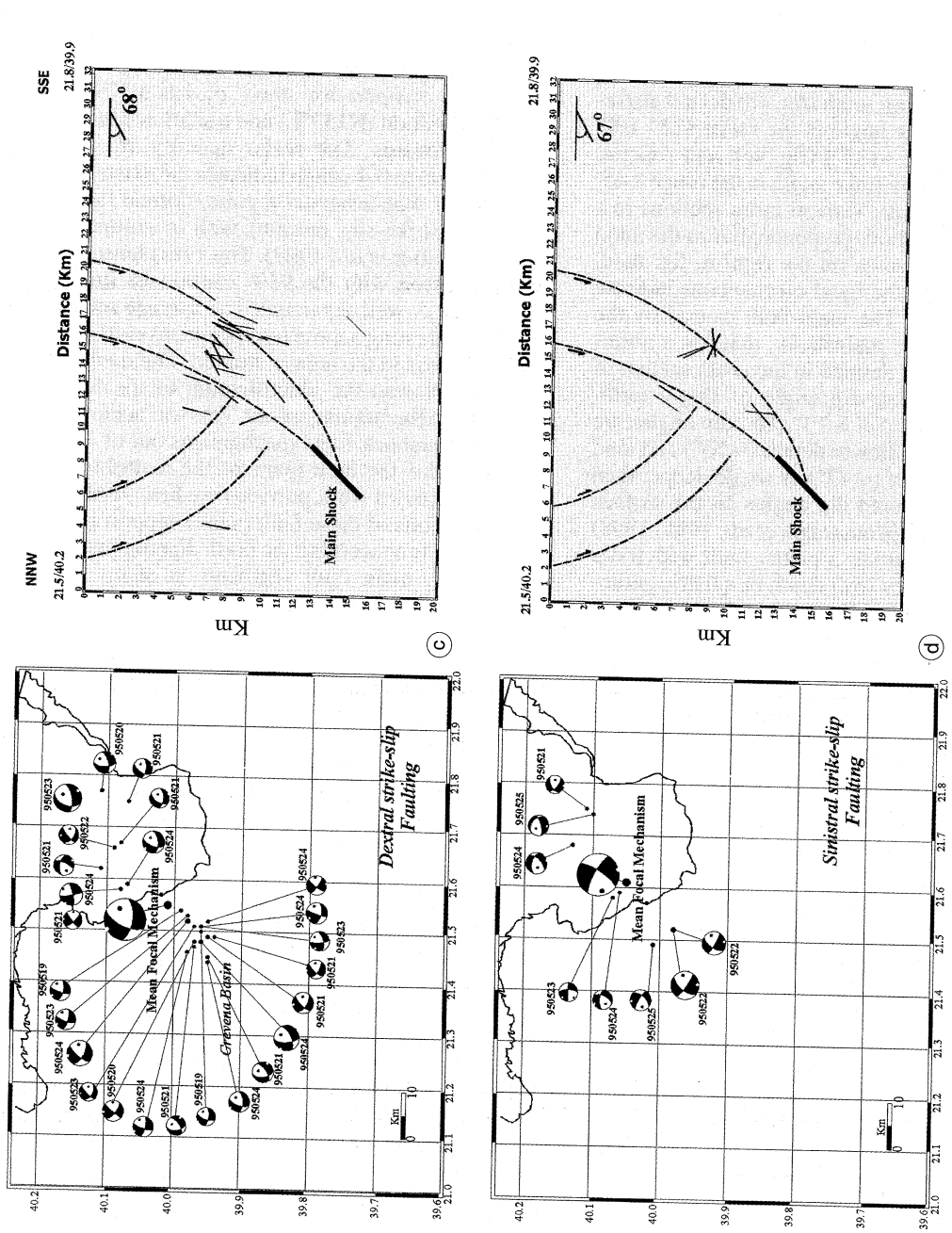

Fig. 4a-d. Focal mechanisms of the earthquakes for which the fault plane could be identified. a) Normal faulting with fault planes dipping north; b) normal faulting with planes dipping south; c) dextral strike-slip faulting; d) sinistral strike-slip faulting. Vertical cross sections in a NNW-SSE direction (perpendicular to the main fault) are also shown in the right side of the figure to indicate the location of the main fault and of the antithetic fault. Normal faulting combined with strong dextral strike-slip motion prevails.

separated in four subsets using the RAKE software (Louvari and Kiratzi, 1997): normal faulting (rake angle $-135°$ up to $-45°$) with fault planes dipping north (fig. 4a); normal faulting with planes dipping south (fig. 4b) dextral strike-slip faulting (rake angle in the range 135°-180° and $-180°$ up to $-135°$) (fig. 4c), and sinistral strike-slip faulting (rake angle in the range $-45°$ up to 45°) (fig. 4d). Vertical cross sections in a NNW-SSE direction (perpendicular to the main fault) are also shown on the right in fig. 4a-d. The majority of the focal mechanisms indicate normal faulting. The main fault caused by the occurrence of the mainshock, that has a northward dip, is well defined in the cross section of fig. 4a. The mean dip angle of these north-dipping planes is 52° ± 13°. The dip angles are sharper in the shallower depths (~ 55°) and tend to become smaller (~ 47°) as we go deeper than 9 km. The measured dip angles on the surface were very large (Mountrakis *et al.*, 1995, 1998) which suggests either a planar fault with a dip angle that changes with depth or a listric geometry. The Chromio-Myrsina antithetic faulting, well observed from the distribution of aftershocks (Hatzfeld *et al.*, 1997, 1998; Papazachos *et al.,* 1998) and the surface traces (Mountrakis *et al.*, 1998), is shown in fig. 4b. The mean dip angle of these south-dipping planes is 43° ± 17°. Figure 4c depicts the dextral strike slip faulting observed at the edges of the main fault scarp along planes that dip at 68° ± 12° northwards. Most of this dextral strike-slip faulting is located at the western edge of the Paleohori Fault, at the area covered by the Grevena basin. Figure 4d shows a few left lateral strike-slip focal mechanisms representing motion along NW-SE striking, probably older, structures prevailing in the area (Pavlides, 1998).

4. Conclusions

The method of Gephart and Forsyth (1984) was used to determine regional stresses in Western Greece using earthquake focal mechanisms from the Kozani-Grevena 1995 earthquake sequence. The results indicate that a single stress tensor is able to explain the fault plane solutions of the aftershocks as well as of the main shock. The data used sample the crust at depths between 4 and 15 km. The maximum compressive stress, σ_1, has a NNE-SSW azimuth (N26°E) and a nearly vertical plunge (80°) while the minimum compressive stress, σ_3, has a NNW-SSE orientation (N159°E) and a shallow plunge (7°) southwards. The scalar quantity, R, was found equal to 0.4 which indicates the existence of a rather transtensional regime (normal faulting with strike-slip motion) with σ_2 compressional (Bellier *et al.*, 1997). The stress tensor is well resolved with the 95% confidence limits for σ_1 and σ_3 well separated. The average misfit is 6.5° indicating a quite homogeneous distribution of stress in the area examined. The method applied allowed the identification of the fault plane from the auxiliary plane. This was achieved for 98 aftershock focal mechanisms out of 177 in total, plus the fault plane of the mainshock, which is known from previous studies. Vertical cross sections of these fault planes support previous results concerning the north dipping (mean dip ~ 52°) main fault segments at sharp dip angles which become smaller as we go deeper than 9 km. The south dipping antithetic faulting was also well identified with planes dipping at ~ 43°. Inversion of GPS measurements yielded a source mechanism consisting of a 43°NW dipping normal fault, with an average slip of 1.2 m and a minimum depth of faulting of 2.8 km (Clarke *et al.*, 1996). In addition SAR interferometry measurements led Meyer *et al.* (1996) to propose a main normal fault between 4 and 15 km depth which branches into small fragments at the surface. All aftershocks are distributed below ~ 5 km depth (Hatzfeld *et al.*, 1997, 1998; Papazachos *et al.*, 1998). On the other hand, we definitely have a fault that has a sharp dip at shallow depths that becomes smoother at its deeper parts. Since the seismicity did not reach shallow depths it is difficult to talk about listric geometry. This depth variable dip angle fault geometry was observed in other normal faulting events in Greece, like the Thessaloniki 1978 earthquake (B. Papazachos *et al.*, 1979; Soufleris and Stewart, 1981) and the Volos (Thessalia) 1980 earthquake (B. Papazachos *et al.*, 1983).

The resolved direction of the extensional stress axis, σ_3, is in good agreement with the NNW-SSE trend of extension in Western Greece

(Pavlides, 1985; Papazachos and Kiratzi, 1996). Almost all of the normal faulting in the area was combined with significant strike-slip motions. The identified fault planes in this work indicate that this strike-slip motion is mainly dextral, along NNE-SSW trending structures, which is the direction of the main neotectonic faults (Pavlides, 1998), while the scarce sinistral strike-slip motion is connected to NW-SE trending pre-existing zones of weakness, a signature of the past compressional phase. Thus, although the faults in the area of Western Greece are activated as normal, however there is a strike-slip component present. This is not observed in Western Greece only, but in Central Macedonia and the Chalkidiki as well (Pavlides *et al.*, 1990). The dextral strike-slip component is dominant in Western Greece, probably connected to the dextral movement of the North Anatolian Fault, which affects the motions. We believe we will see the limits of these strike-slip motions in a future work by applying the stress inversion method to the Aegean and the surrounding lands as a whole.

The limited sinistral strike-slip motions are along NW-SE trending structures inherited from previous deformations. In conclusion, the complexity of the fault geometry is the result of the superimposition of the young extensional tectonics on the mature well-developed old thrust faults of Central Hellenides. As Chiarabba and Selvaggi (1997) point out, the active stress field generates normal faults and basins perpendicular to the preexisting thrust belt. The reactivation of these thrusts that are favorably oriented with the regional stress is a mechanism that probably controls the seismotectonic evolution of Western Greece.

Acknowledgements

The author would like to thank Dr. Salvatore Spampinato from the University of Catania for help with the computer codes, Eleni Louvari for help with some of the figures and Assoc. Prof. S. Pavlides for stimulating discussions. Partial support from the Science for Peace Programme (Project 972342) is highly appreciated.

REFERENCES

BELLIER, O., S. OVER, A. POISSON and J. ANDRIEUX (1997): Recent temporal change in the stress state and modern stress field along the North Anatolian Fault Zone (Turkey), *Geophys. J. Int.*, **131**, 61-86.

CHIARABBA, C. and G. SELVAGGI (1997): Structural control on fault geometry: example of the Grevana M_s 6.6, normal faulting earthquake, *J. Geophys. Res.*, **102**, 22445-22457.

CLARKE, P., D. PARADISIS, P. BRIOLE, P. ENGLAND, B. PARSONS, H. BILLIRIS, G. VEIS and J.-C. RUEGG (1996): Geodetic investigation of the 13 May 1995 Kozani-Grevena (Greece) earthquake, *Geophys. Res. Lett.*, **24**, 707-710.

GEPHART, J. (1990): Stress and the direction of slip on fault planes, *Tectonics*, **9**, 845-858.

GEPHART, J. and W. FORSYTH (1984): An improved method for determining the regional stress tensor using earthquake focal mechanism data: applications to the San Fernando earthquake sequence, *J. Geophys. Res.*, **89**, 9305-9320.

HATZFELD, D., V. KARAKOSTAS, M. ZIAZIA, G. SELVAGGI, S. LEBORGNE, C. BERGE, R. GUIGUET, A. PAUL, PH. VOIDOMATIS, D. DIAGOURTAS, I. KASSARAS, I. KOUTSIKOS, K. MAKROPOULOS, R. AZZARA, M. DI BONA, S. BACCHECHI, P. BERNARD and CH. PAPAIOANNOU (1997): The Kozani - Grevena (Greece) earthquake of May 13, 1995, revisited from a detailed seismological study, *Bull. Seismol. Soc. Am.*, **87**, 463-473.

HATZFELD, D., V. KARAKOSTAS, M. ZIAZIA, G. SELVAGGI, S. LEBORGNE, C. BERGE and K. MAKROPOULOS (1998): The Kozani-Grevena (Greece) earthquake of May 13, 1995, a seismological study, *J. Geodyn.*, **26**, 245-254.

LOUVARI, E. and A. KIRATZI (1997): Rake: a window's program to plot earthquake focal mechanisms and stress orientation, *Comput. Geosci.*, **23**, 851-857.

MEYER, B., R. ARMIJO, D. MASSONNET, J-B. DE CHABALIER, C. DELACOURT, J-C. RUEGG, J. ACACHE, P. BRIOLE and D. PAPANASTASSIOU (1996): The Grevena (Northern Greece) earthquake: fault model constrained with tectonic observations and SAR interferometry, *Geophys. Res. Lett.*, **23**, 2677-2680.

MICHAEL, A. (1987): Use of focal mechanisms to determine stress: a control study, *J. Geophys. Res.*, **92**, 357-368.

MOUNTRAKIS, D. (1986): The Pelagonian zone in Greece: a polyphase deformed fragment of the Cimmerian continent and its role in the geotectonic evolution of East Mediterranean, *J. Geology* , **94**, 335-347.

MOUNTRAKIS, D., S. PAVLIDES, N. ZOUROS, A. CHATZIPETROS and D. KOSTOPOULOS (1995): The 13 May 1995 Western Macedonia (Greece) earthquake. Preliminary results on the seismic fault geometry and kinematics, in *Proceedings of the XV Congress of the Carpatho-Balkan Geological Association, September 17-20, 1995, Athens, Greece,* 112-121.

MOUNTRAKIS, D., S. PAVLIDES, N. ZOUROS, T. ASTARAS and A. CHATZIPETROS (1998): Seismic fault geometry and kinematics of the 13 May 1995 Western Macedonia (Greece) earthquake, *J. Geodyn.*, **26**, 175-196.

PAPANASTASSIOU, D., G. DRAKATOS, N. VOULGARIS and G. STAVRAKAKIS (1998): The May 13, 1995, Kozani-Grevena (NW Greece) earthquake: source study and its tectonic implications, *J. Geodyn.*, **26**, 233-244.

PAPAZACHOS, B.C. and C.B. PAPAZACHOU (1997): *The Earthquakes of Greece* (Ziti Publications, Thessaloniki, Greece), pp. 304.

PAPAZACHOS, B., D. MOUNTRAKIS, A. PSILOVIKOS and G. LEVENTAKIS (1979): Surface fault traces and fault plane solutions of May-June 1978 major shocks in the Thessaloniki area, *Tectonophysics,* **53**, 171-183.

PAPAZACHOS, B., D. PANAGIOTOPOULOS, T. TSAPANOS, D. MOUNTRAKIS and G. DIMOPOULOS (1983): A study of the 1980 summer seismic sequence in the Magnesia region of Central Greece. *Geophys. J. R. Astron. Soc.,* **75**, 155-168.

PAPAZACHOS, B.C, D.G. PANAGIOTOPOULOS, E.M. SCORDILIS, G.F. KARAKAISIS, CH.A. PAPAIOANNOU, B.G. KARAKOSTAS, E.E. PAPADIMITRIOU, A.A. KIRATZI, P.M. HATZIDIMITRIOU, G.N. LEVENTAKIS, PH. S. VOIDOMATIS, K.J. PEFTITSELIS and T.M. TSAPANOS (1995): Focal properties of the 13 May 1995 large (M_s = 6.6) earthquake in the Kozani area (North Greece), in *Proceedings of the XV Congress of the Carpatho-Balkan Geological Association, September 17-20, 1995, Athens, Greece*, 96-106.

PAPAZACHOS, B.C, B.G. KARAKOSTAS, A.A. KIRATZI, E.E. PAPADIMITRIOU and C. PAPAZACHOS (1998): A model for the Kozani-Grevena seismic sequence, *J. Geodyn.*, **26**, 217-231.

PAPAZACHOS, C.B. and A.A. KIRATZI (1996). A detailed study of the active crustal deformation in the Aegean and surrounding area, *Tectonophysics*, **253**, 129-153.

PAPAZACHOS, C.B., B.G. KARAKOSTAS and E.M. SCORDILIS (1998): Crustal and upper mantle structure of the Kozani-Grevena and surrounding area obtained by non-linear inversion of *P* and *S* travel times, *J. Geodyn.*, **26**, 217-231.

PARKER, R. and M. MCNUTT (1980): Statistics for the one-norm misfit measure, *J. Geophys. Res.,* **85**, 4429-4430.

PAVLIDES, S. (1985): Neotectonic evolution of the Florina-Vegoritis-Ptolemais basin (W. Macedonia, Greece), *Ph. D. Thesis*, University of Thessaloniki, pp. 265 (in Greek).

PAVLIDES, S. (1998): Geologic faults and earthquakes: investing the seismogenetic fault that caused the Kozani-Grevena 1995 seismic sequence, in *Proceedings of the Internationl Conference «The Kozani-Grevena Earthquake of 13 May 1995: a Scientific and Social Approach»*, 169-181 (in Greek).

PAVLIDES, S. and G. KING (Editors) (1998): The 1995 Kozani-Grevena earthquake (N. Greece): an introduction, in *Results of the May 13, 1995 Kozani-Grevena Earthquake – Inqua Neotectonic Commission Parallel Session on Earthquake Geology, J. Geodyn.,* **26** (special issue), 171-173.

PAVLIDES, S. and D. MOUNTRAKIS (1987): Extensional tectonics of Northwestern Macedonia, Greece, since the Late Miocene, *J. Struct. Geol.* **9**, 385-392.

PAVLIDES, S. and K. SIMEAKIS (1988): Neotectonic and active tectonics in low seismicity areas of Greece: Vegoritis (NW Macedonia) and Melos Isl. complex (Cyclades) – Comparison, *Ann. Geol. Pays Hellenique*, **33**, 161-176.

PAVLIDES, S., D. MOUNTRAKIS, A. KILIAS and M. TRANOS (1990). The role of strike-slip movements in the extensional area of Northern Aegean (Greece). A case of transtensional tectonics, *Ann. Tectonicae,* **4**, 196-211.

PAVLIDES, S.B., N.C. ZOUROS, A.A. CHATZIPETROS, D.S. KOSTOPOULOS and D.M. MOUNTRAKIS (1995): The 13 May 1995 Western Macedonia, Greece (Kozani Grevena) earthquake; preliminary results, *Terra Nova*, **7**, 544-549.

SOUFLERIS, C. and G. STEWART (1981): A source study of the Thessaloniki (N. Greece) 1978 earthquake sequence, *Geophys. J. R. Astron. Soc.,* **67**, 343-358.

STIROS, S. (1998). Historical seismicity, paleoseismicity and seismic risk in Western Macedonia, Northern Greece, *J. Geodyn.*, **26**, 271-287.

WYSS, M., B. LIANG, W. TANIGAWA and W. XIAOPING (1992): Comparison of orientations of stress and strain tensor based on fault plane solutions in Kaoiki, Hawaii, *J. Geophys. Res.*, **97**, 4769-4790.

(received March 10, 1999;
accepted June 9, 1999)